

# Intracellular Alkalinization Induces Cytosolic $\text{Ca}^{2+}$ Increases by Inhibiting Sarco/Endoplasmic Reticulum $\text{Ca}^{2+}$ -ATPase (SERCA)

Sen Li, Baixia Hao, Yingying Lu, Peilin Yu, Hon-Cheung Lee, Jianbo Yue\*

Department of Physiology, University of Hong Kong, Hong Kong, China

## Abstract

Intracellular pH (pHi) and  $\text{Ca}^{2+}$  regulate essentially all aspects of cellular activities. Their inter-relationship has not been mechanistically explored. In this study, we used bases and acetic acid to manipulate the pHi. We found that transient pHi rise induced by both organic and inorganic bases, but not acidification induced by acid, produced elevation of cytosolic  $\text{Ca}^{2+}$ . The sources of the  $\text{Ca}^{2+}$  increase are from the endoplasmic reticulum (ER)  $\text{Ca}^{2+}$  pools as well as from  $\text{Ca}^{2+}$  influx. The store-mobilization component of the  $\text{Ca}^{2+}$  increase induced by the pHi rise was not sensitive to antagonists for either  $\text{IP}_3$ -receptors or ryanodine receptors, but was due to inhibition of the sarco/endoplasmic reticulum  $\text{Ca}^{2+}$ -ATPase (SERCA), leading to depletion of the ER  $\text{Ca}^{2+}$  store. We further showed that the physiological consequence of depletion of the ER  $\text{Ca}^{2+}$  store by pHi rise is the activation of store-operated channels (SOCs) of Orai1 and Stim1, leading to increased  $\text{Ca}^{2+}$  influx. Taken together, our results indicate that intracellular alkalinization inhibits SERCA activity, similar to thapsigargin, thereby resulting in  $\text{Ca}^{2+}$  leak from ER pools followed by  $\text{Ca}^{2+}$  influx via SOCs.

**Citation:** Li S, Hao B, Lu Y, Yu P, Lee H-C, et al. (2012) Intracellular Alkalinization Induces Cytosolic  $\text{Ca}^{2+}$  Increases by Inhibiting Sarco/Endoplasmic Reticulum  $\text{Ca}^{2+}$ -ATPase (SERCA). PLoS ONE 7(2): e31905. doi:10.1371/journal.pone.0031905

**Editor:** Silvia N. Moreno, University of Georgia, United States of America

**Received:** August 22, 2011; **Accepted:** January 19, 2012; **Published:** February 27, 2012

**Copyright:** © 2012 Li et al. This is an open-access article distributed under the terms of the Creative Commons Attribution License, which permits unrestricted use, distribution, and reproduction in any medium, provided the original author and source are credited.

**Funding:** This work was supported by Research Grant Council (RGC) grants (HKU 784710M, HKU 782709M, HKU 785911M), a National Natural Science Foundation of China (NSFC)/RGC grant from Hong Kong (N\_HKU 737/09), and a Special Fellow Award from the Leukemia and Lymphoma Society of America (Dr. Yue). The funders had no role in study design, data collection and analysis, decision to publish, or preparation of the manuscript.

**Competing Interests:** The authors have declared that no competing interests exist.

\* E-mail: jyue@hku.hk

## Introduction

The activity of virtually all proteins and macromolecules can be modulated by protons; thus intracellular pH (pHi) is rigorously regulated for survival [1,2,3]. Subtle and transient pHi changes occur under many physiological conditions. For examples, activity-dependent membrane depolarization elevates pHi in astrocytes of rat cortex [4]. Likewise, both capacitation of spermatozoa [5] and fertilization of eggs [6], induce intracellular alkalinization. Much greater and sustained pHi changes, on the other hand, can occur under pathological conditions, e.g. acidification of pHi during apoptosis and alkalinization in tumorigenesis [2]. Cells passively stabilize pHi by the buffering capacity of a variety of intracellular weak acids and bases, especially  $\text{HCO}_3^-$ , generated by  $\text{CO}_2$  hydration and subsequent deprotonation of carbonic acid. However, these intrinsic buffering systems can be overpowered during continued extra- and intracellular stress or stimulation. Cells, therefore, have evolved a complicated proton transporting system to regulate cytosolic pH as well as the pH in other cellular compartments [1].

Under physiological conditions, cells utilize two major pH-regulatory ion transporters at the plasma membrane, the  $\text{Na}^+$ - $\text{H}^+$ -exchangers (NHEs) and the  $\text{Na}^+$ - $\text{HCO}_3^-$  co-transporters (NBCs), to extrude the protons produced during normal cellular metabolic activity. Some cells also utilize  $\text{Na}^+$ -dependent  $\text{Cl}^-$ - $\text{HCO}_3^-$  exchangers (NDCBEs) or monocarboxylate- $\text{H}^+$  co-transporters (MCTs) for similar purposes. On the other hand, activation of the

$\text{Cl}^-$ - $\text{HCO}_3^-$  anion exchanger (AEs) and plasma membrane  $\text{Ca}^{2+}$ -ATPase (PMCA) can lead to cytosolic acidification. Among all of these transporters, NHE1 is perhaps the most dominant one for maintaining pHi homeostasis [1,2]. Its activity is not only modulated by cytosolic  $\text{H}^+$ , but also by various extra- or intracellular signals, leading to elevation of pHi during diverse cellular processes, such as autophagy, migration, adhesion, chemotaxis, and cell cycle progression [2,7,8].

Likewise,  $\text{Ca}^{2+}$  is equally important in regulating diverse cell functions, including fertilization, cell proliferation and differentiation [9]. Cytosolic  $\text{Ca}^{2+}$  level at rest is kept low mainly by the active extrusion of cytosolic  $\text{Ca}^{2+}$  out of cells via the PMCA and the  $\text{Na}^+$ / $\text{Ca}^{2+}$ -exchanger, as well as by sequestration of  $\text{Ca}^{2+}$  into the endoplasmic reticulum (ER) and mitochondria via a sarco/endoplasmic reticulum  $\text{Ca}^{2+}$ -ATPase (SERCA) and a mitochondrial  $\text{Ca}^{2+}$  uniporter, respectively. External signaling can markedly increase cytosolic  $\text{Ca}^{2+}$  levels by opening plasma membrane ion channels, such as voltage-gated  $\text{Ca}^{2+}$ -selective channels (CaVs) and transient receptor potential (TRP) ion channels. Cytosolic  $\text{Ca}^{2+}$  concentration can also be suddenly and dramatically increased by release from the ER  $\text{Ca}^{2+}$  store, through activation of  $\text{IP}_3$  receptors ( $\text{IP}_3$ Rs) and ryanodine receptors (RyRs) in ER [10]. At least three endogenous  $\text{Ca}^{2+}$  mobilizing messengers have been identified for regulating these  $\text{Ca}^{2+}$  release channels, which include inositol trisphosphate ( $\text{IP}_3$ ), nicotinic acid adenine dinucleotide phosphate (NAADP), and cyclic adenosine diphosphoribose (cADPR).  $\text{Ca}^{2+}$  influx and internal  $\text{Ca}^{2+}$  store release

are normally interconnected. Thus, depletion of the ER Ca<sup>2+</sup> store can trigger activation of the store-operated channels (SOCs) at the plasma membrane, mediated by Orails and Stims, and lead to Ca<sup>2+</sup> influx [11].

Intracellular alkalinization has been linked to intracellular Ca<sup>2+</sup> events. Intracellular Ca<sup>2+</sup> spikes that occur during oocyte maturation and egg fertilization in several marine invertebrate and amphibian species are believed to be responsible for regulating the subsequent alkalinization of pHi [12]. Conversely, intracellular alkalinization occurring during the initiation of sperm motility and the activation of the acrosome reaction can likewise regulate Ca<sup>2+</sup> uptake [5,13]. In vertebrates, intracellular alkalinization can indeed increase Ca<sup>2+</sup> current in a wide variety of cells and tissues, including various types of neurons [14,15], rat pancreatic acinar cells [16], different types of muscle cells [17], mast cells [18], aortic endothelial cells [19], and lymphocytes [20]. Different membrane Ca<sup>2+</sup> channels are involved in alkaline pHi-triggered Ca<sup>2+</sup> entry depending on cell or tissue types [5,15,21,22], which have been well documented. However, the studies on the mechanism of alkaline pHi triggered internal Ca<sup>2+</sup> release are sparse and conflicting, especially concerning whether or how IP<sub>3</sub> signaling is required [19,23,24].

Here we studied the mechanisms underlying intracellular alkalinization-induced cytosolic Ca<sup>2+</sup> changes in various cell lines. We demonstrated that intracellular alkalinization inhibits SERCA activity, leading to Ca<sup>2+</sup> leak from the ER. The depletion of ER Ca<sup>2+</sup> stores then activates Ca<sup>2+</sup> influx through SOCs of Stim1 and Orail.

## Results

### Intracellular alkalinization induces cytosolic Ca<sup>2+</sup> increase

It has been shown previously that weak bases, such as ammonium chloride (NH<sub>4</sub>Cl) or methylamine, can induce cytosolic Ca<sup>2+</sup> increase (reviewed in Ref. [3]). However, the high concentrations of these bases used in these studies complicated the interpretation of the results due to osmolarity changes or impurity of the compounds. In the process of synthesizing cell permeant analogs of the Ca<sup>2+</sup> releasing messengers IP<sub>3</sub>, NAADP, and cADPR, we found the hydrobromide salt of diisopropylethyl amine (DIEA.HBr), an organic base commonly used in the organic chemistry, can induce cytosolic Ca<sup>2+</sup> increases, similar to that of NH<sub>4</sub>Cl, in a dose dependent manner, whereas sodium acetate, a weak acid, failed to change Ca<sup>2+</sup> (Figure 1A). We purified DIEA.HBr by HPLC and crystallization (Figure S1). Controls showed that neither NaBr nor KBr could induce any cytosolic Ca<sup>2+</sup> changes (Figure S2). In addition, DIEA.HBr induced cytosolic pH increase in a dose dependent manner in HeLa cells (Figure S3). As shown in Figures 1B and 1C, the pH rise triggered by DIEA.HBr or NH<sub>4</sub>Cl preceded the cytosolic Ca<sup>2+</sup> increase. Moreover, administration of weak acids, such as sodium acetate, markedly inhibited the ability of DIEA.HBr or NH<sub>4</sub>Cl to induce intracellular alkalinization and cytosolic Ca<sup>2+</sup> rises. Similar results have been observed in various cell lines, showing generality (Figure S4). These results thus indicate that intracellular alkalinization induces cytosolic Ca<sup>2+</sup> increase.

### Intracellular alkalinization induces Ca<sup>2+</sup> release from ER Ca<sup>2+</sup> pools independent of IP<sub>3</sub> receptors and ryanodine receptors

Next, we traced the sources of the cytosolic Ca<sup>2+</sup> increases induced by these bases. Since treatment of a variety of cell types with NH<sub>4</sub>Cl or DIEA.HBr basically generated similar results, only the data of DIEA.HBr in HeLa cells, PC12 cells, and NIH 3T3

cells were presented in the remainder of the results section. Pretreatment with thapsigargin, a specific SERCA inhibitor, completely abolished DIEA.HBr-induced Ca<sup>2+</sup> changes in HeLa cells, and the inclusion of EGTA in a Ca<sup>2+</sup> free medium markedly diminished the Ca<sup>2+</sup> peaks of the sustained phase (Figure 2A). Similar results have been observed in NIH3T3 cells and PC12 cells (Figure S4). These results indicate that intracellular alkalinization induces Ca<sup>2+</sup> release from ER pools, which is followed by extracellular Ca<sup>2+</sup> influx. Interestingly, treatment of HeLa cells with *Xestospongin C* (*XeC*), an IP<sub>3</sub>R antagonist, or U73122, a specific inhibitor of phospholipase C, had little effect on cytosolic Ca<sup>2+</sup> increases induced by DIEA.HBr (Figure 2B). In contrast, *XeC* or U73122 effectively inhibited histamine-induced Ca<sup>2+</sup> increases in HeLa cells (Figure S5A). Similar data have also been observed in several other cell lines (data not shown). These data indicate that the Ca<sup>2+</sup> release from ER induced by intracellular alkalinization is independent of IP<sub>3</sub>Rs. In addition, no RyRs were detected in HeLa cells and HeLa cells were not responsive to caffeine treatment (data not shown and Figure S5B), suggesting that intracellular alkalinization-induced Ca<sup>2+</sup> increases in HeLa cells is also independent of RyRs. Indeed, a high concentration of ryanodine, acting as a RyRs antagonist, or 8-Br-cADPR, a cADPR antagonist, had little effect on cytosolic Ca<sup>2+</sup> increases induced by DIEA.HBr in PC12 cells (Figure 2C), whereas this concentration of ryanodine effectively inhibited caffeine-induced Ca<sup>2+</sup> increases in PC12 cells (Figure S5B). We have also previously shown that 8-Br-cADPR can effectively block Ca<sup>2+</sup> increases induced by cADPR, which reportedly mobilizes Ca<sup>2+</sup> via RyRs from ER, in PC12 cells [25]. Similar results have been observed in several other RyRs-expressing cell lines (data not shown). These results document that the Ca<sup>2+</sup> release from ER induced by intracellular alkalinization is independent of RyRs as well.

### Intracellular alkalinization induces cytosolic Ca<sup>2+</sup> increase independent of acid Ca<sup>2+</sup> store

To test whether the acidic Ca<sup>2+</sup> store is affected by intracellular alkalinization, we treated HeLa cells with glycyl-L-phenylalanine 2-naphthylamide (GPN) to selectively disrupt the lysosomal membrane [26], and released the lysosomal Ca<sup>2+</sup> [27]. As shown in Figure S6, 50 μM GPN completely depleted the lysosomal Ca<sup>2+</sup> pools, evidenced by the fact that subsequent addition of GPN (50 μM) or bafilomycin A1 (0.5 μM), a specific inhibitor of the vacuolar-type H(+)-ATPase that is known to be able to release Ca<sup>2+</sup> from the lysosomes normally, failed to release any more Ca<sup>2+</sup>. In contrast, pretreating cells with GPN failed to significantly alter the DIEA.HBr-induced Ca<sup>2+</sup> rise in HeLa cells (Figure 2D), indicating that the Ca<sup>2+</sup> pools targeted by DIEA.HBr are not the lysosomes.

### Intracellular alkalinization releases Ca<sup>2+</sup> from ER by lowering SERCA activity

The kinetics of Ca<sup>2+</sup> release from ER by intracellular alkalinization markedly differed from that induced by histamine, which is known to be mediated by IP<sub>3</sub>Rs, whereas it is similar to the thapsigargin-triggered Ca<sup>2+</sup> release (Figure 3A). Thapsigargin blocks SERCA and thereby allows Ca<sup>2+</sup> leak from the ER into the cytosol. Since SERCA activity is known to be pH-dependent in vitro [28,29] and SERCA ATPase activities in alkaline buffers were significantly lower than that in neutral pH buffer (Figure S7), we speculated that intracellular alkalinization might release Ca<sup>2+</sup> from ER by inhibiting SERCA activity as well. We, therefore, examined the ER Ca<sup>2+</sup> content in HeLa cells at varied time points

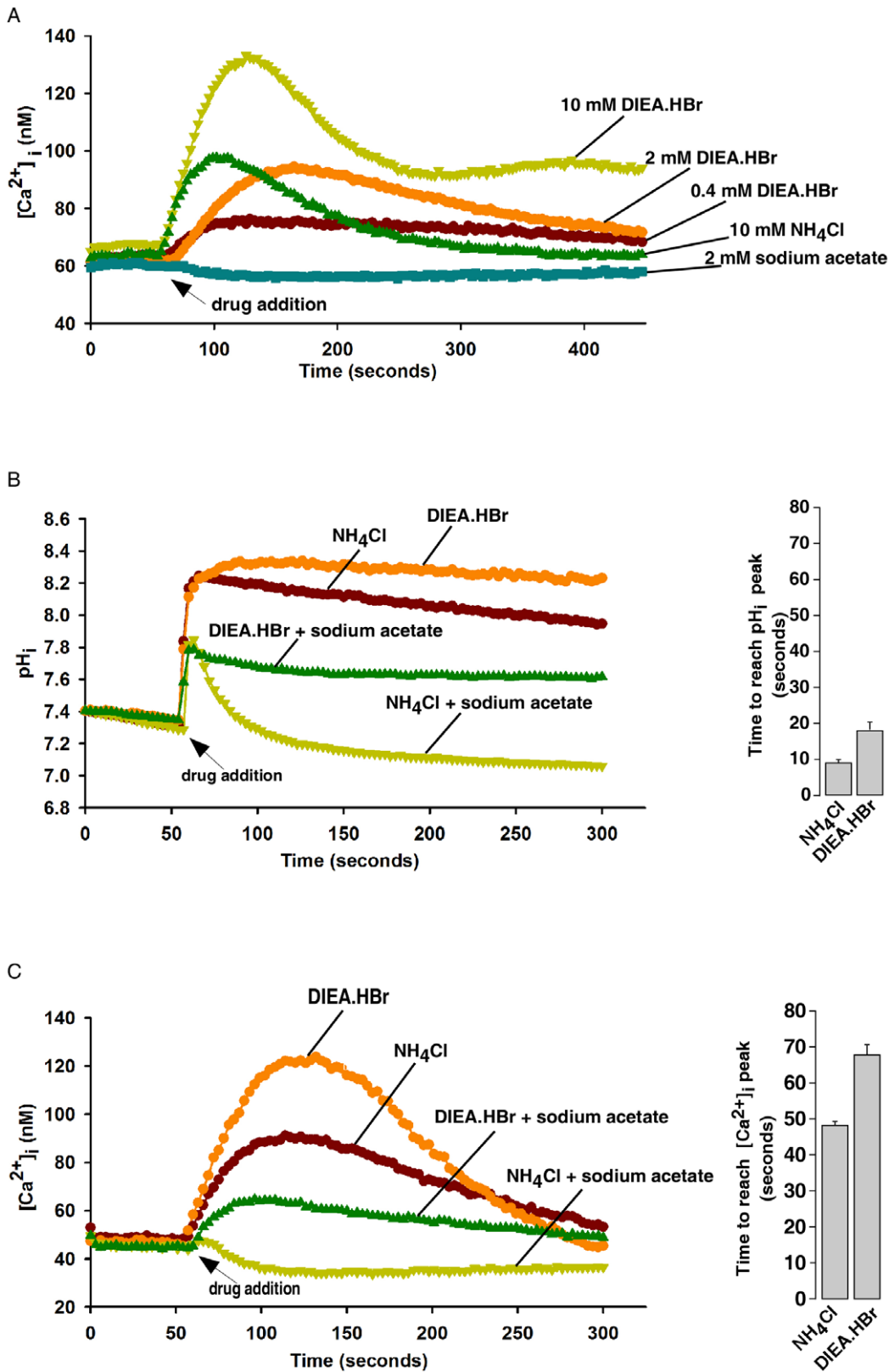


**Figure 1. Intracellular alkalinization induces cytosolic Ca<sup>2+</sup> increases in HeLa cells.** (A) DIEA.HBr, similar to NH<sub>4</sub>Cl, induced cytosolic Ca<sup>2+</sup> increases in a dose-dependent manner in HeLa cells as measured by the Ca<sup>2+</sup>-indicator, Fura-2 AM. (B) Intracellular alkalinization induced by DIEA.HBr (10 mM) and NH<sub>4</sub>Cl (10 mM) were inhibited by sodium acetate (40 mM) as measured by the pH-indicator, BCECF AM. (C) Cytosolic Ca<sup>2+</sup> increases induced by DIEA.HBr (10 mM) and NH<sub>4</sub>Cl (10 mM) were markedly inhibited by sodium acetate (40 mM). The graphs represent data from three independent experiments. Data quantifications of the time to reach pH<sub>i</sub> peak (B) or [Ca<sup>2+</sup>]<sub>i</sub> peak (C) after drug treatment were expressed as mean ± S.E., n = 30–50 cells.

doi:10.1371/journal.pone.0031905.g001

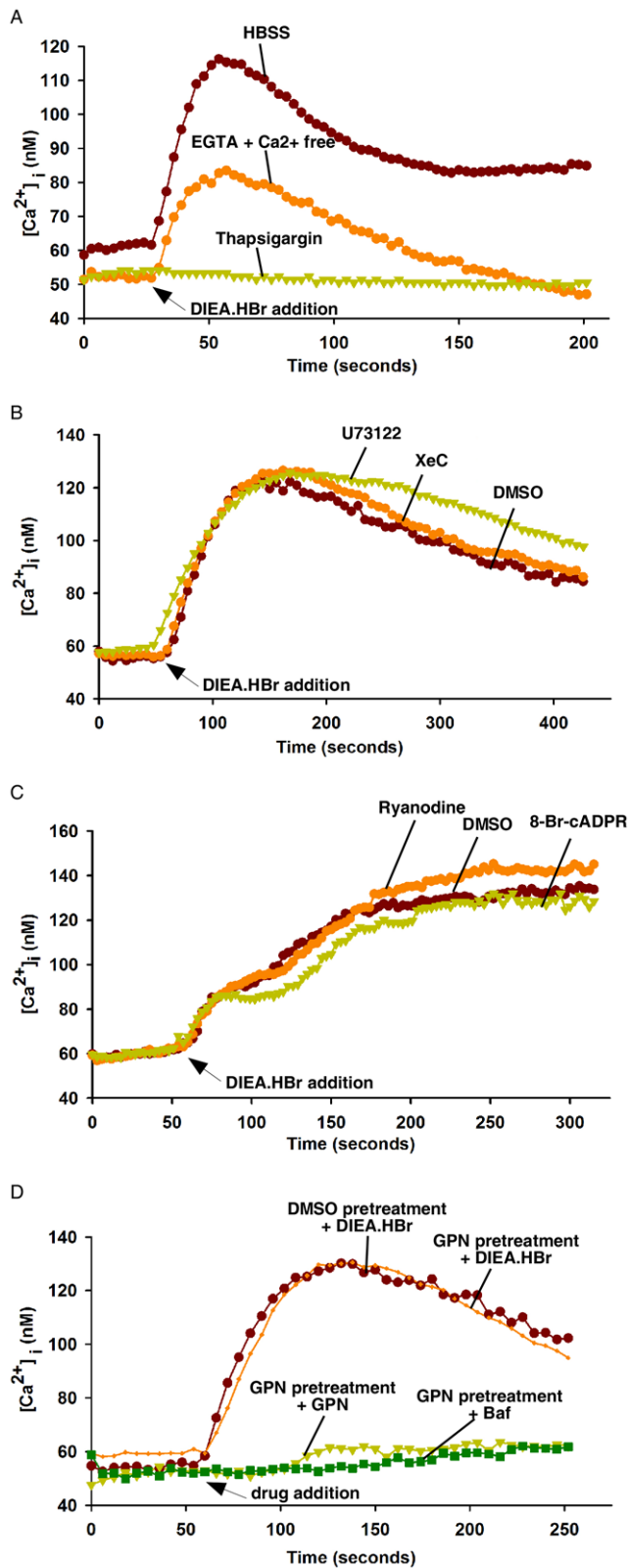


**Figure 2. Intracellular alkalinization releases Ca<sup>2+</sup> from ER pools in HeLa cells and PC12 cells.** (A) DIEA.HBr (4 mM)-induced Ca<sup>2+</sup> increase in Fura-2 loaded HeLa cells was abolished by thapsigargin (1 μM) pretreatment. This Ca<sup>2+</sup> increase was inhibited by removal of external Ca<sup>2+</sup> (Ca<sup>2+</sup>-free HBSS with 4 mM EGTA). (B) Pretreatment of Fura-2 loaded HeLa cells with either *Xestospongin C* (XeC) (10 μM) or U73122 (10 μM) did not inhibit the DIEA.HBr-induced Ca<sup>2+</sup> increase

compared with untreated cells. The graphs represent data from three independent experiments. (C) Pretreatment of Fura-2 loaded PC12 cells with ryanodine (20 μM) or 8-Br-cADPR (100 μM) did not inhibit the DIEA.HBr-induced Ca<sup>2+</sup> increase compared with untreated cells. The graphs represent data from three independent experiments. (D) Pretreatment of Fura-2 loaded HeLa cells with glycyl-L-phenylalanine 2-naphthylamide (GPN) (50 μM) did not inhibit the DIEA.HBr-induced Ca<sup>2+</sup> increase compared with untreated cells while completely blocked GPN or bafilomycin A1 (0.5 μM)-induced Ca<sup>2+</sup> increase. The graphs represent data from three independent experiments. doi:10.1371/journal.pone.0031905.g002

after pretreatment with DIEA.HBr or NH<sub>4</sub>Cl. The peak value of thapsigargin-induced cytosolic Ca<sup>2+</sup> currents is commonly used as an index for ER Ca<sup>2+</sup> content [30]. As shown in Figure 3B, NH<sub>4</sub>Cl or DIEA.HBr abruptly increased pHi to similar levels, which were followed by a slower return to basal value. The kinetics of the pHi-return in the DIEA.HBr-treated cells was much slower than that in NH<sub>4</sub>Cl treated cells. Accordingly, pretreatment of HeLa cells with either base markedly reduced the amplitudes of thapsigargin induced Ca<sup>2+</sup> rise, with the inhibitory extents correlating with the pHi value induced by either base in a time dependent manner (Figure 3C). On the other hand, pretreatment of cells with a weak acid, sodium acetate, or incubating cells in a Ca<sup>2+</sup> free medium, or pretreatment of cells with ATP, had little effect on thapsigargin-induced Ca<sup>2+</sup> release from ER. Similarly, intracellular alkalinization also inhibited the amplitude of ionomycin-induced Ca<sup>2+</sup> release in a Ca<sup>2+</sup> free medium (Figure S8). These results indicate that intracellular alkalinization reduces the ER Ca<sup>2+</sup> contents.

To demonstrate that the reduction of ER Ca<sup>2+</sup> content by intracellular alkalinization was through inhibition of the SERCA, Ca<sup>2+</sup> uptake experiments were performed. Saponin permeabilized HeLa cells were incubated in an uptake medium buffered at different pH values, and the Ca<sup>2+</sup> concentration in the medium was measured by Fluo-3. The decay of Fluo-3 fluorescent signal over time is an indicator of Ca<sup>2+</sup> uptake back into the ER and thus reflects the SERCA activity (Figure 3D) [31]. The addition of thapsigargin in the neutral uptake medium completely abolished Ca<sup>2+</sup> uptake, indicating that SERCA was solely responsible for the Ca<sup>2+</sup> uptake. Consistently, the decay of Fluo-3 intensity at alkaline pH (pH 8.0) was markedly inhibited as compared to that in neutral (pH 7.2) or acidic (pH 6.4) media (Figure 3D). Addition of thapsigargin to cells in an alkaline pH medium also completely abolished the remaining Ca<sup>2+</sup> uptake. Similar results have also been observed in uptake buffer containing ruthenium red to exclude the possibility of Ca<sup>2+</sup> uptake into mitochondria (Figure S9). All these data indicated that SERCA activity was inhibited, at least partially, in alkaline medium.

To further demonstrate that intracellular alkalinization inhibits SERCA activity, we examined the effects of intracellular alkalinization on sequestration of cytosolic Ca<sup>2+</sup> to ER following Ca<sup>2+</sup> release triggered by histamine or ATP in HeLa cells. In the absence of extracellular Ca<sup>2+</sup>, histamine releases Ca<sup>2+</sup> from the ER into the cytosol via the IP<sub>3</sub>Rs, and SERCA then pumps the cytosolic Ca<sup>2+</sup> back to the ER and returns the cytosolic Ca<sup>2+</sup> to the basal levels. Thapsigargin abolishes SERCA activity, thereby greatly decreasing the decay rate of the cytosolic Ca<sup>2+</sup>. As showed in Figure 4A, the decay rate after histamine induced Ca<sup>2+</sup> release was 11.1 ± 0.9 nM/second (n = 36 cells), while this rate decreased to 4.9 ± 0.3 nM/second (n = 29) in the presence of 10 μM thapsigargin. Similarly, the decay rate of histamine in the presence of DIEA.HBr was 5.8 ± 0.4 nM/second (n = 9), which was also significant lower than that of histamine alone. Moreover, the effects of intracellular alkalinization on the decay rate of cytosolic Ca<sup>2+</sup> after histamine treatment were examined in the presence of

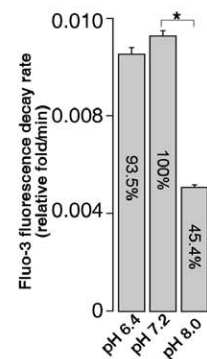
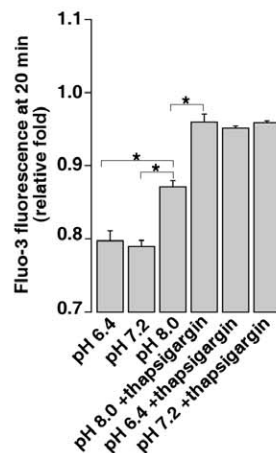
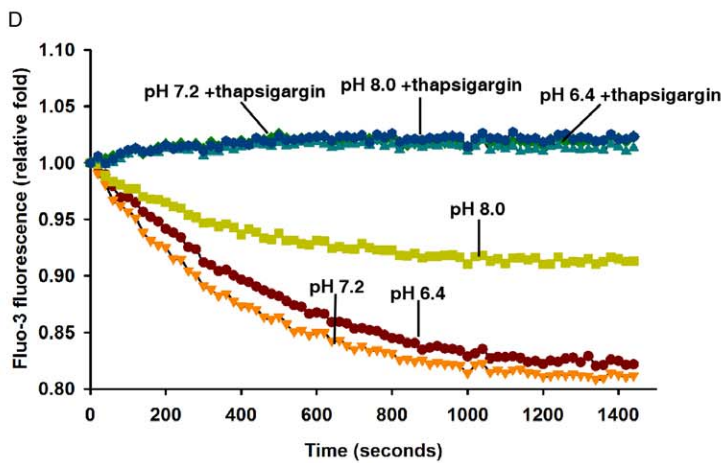
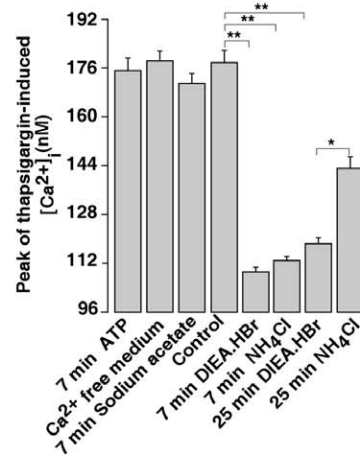
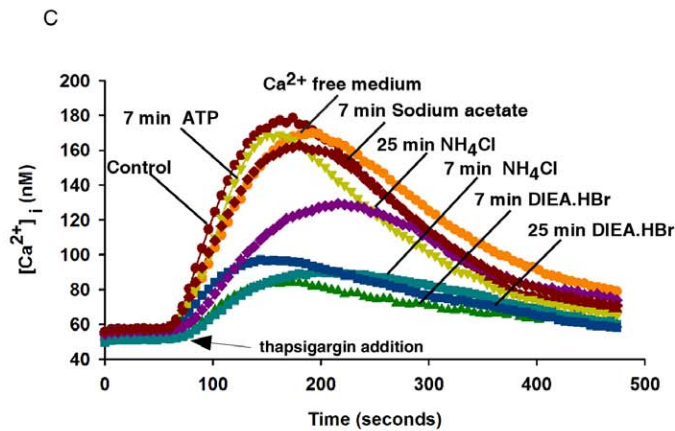
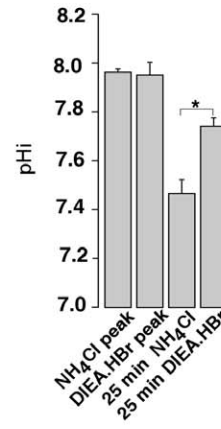
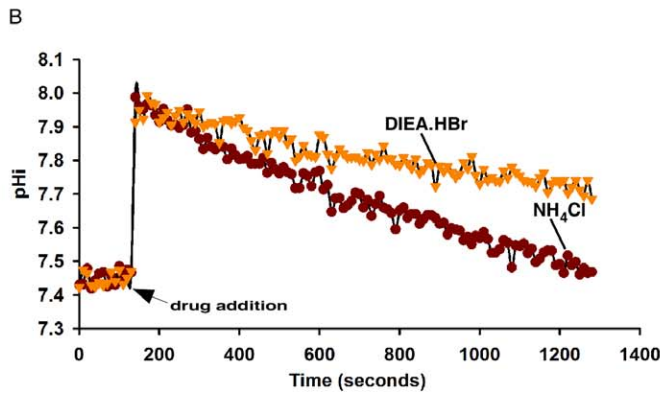
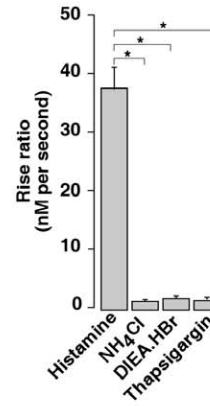
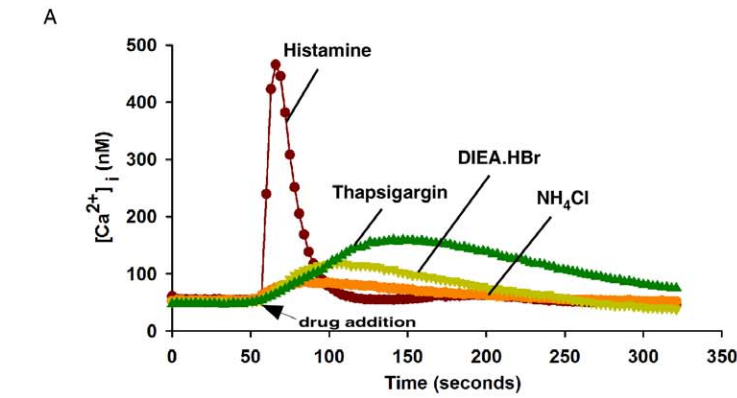


**Figure 3. Intracellular alkalinization inhibits ER SERCA activity in HeLa cells.** (A) Kinetics of cytosolic Ca<sup>2+</sup> increases induced by histamine (10 μM), NH<sub>4</sub>Cl (4 mM), DIEA.HBr (4 mM), and thapsigargin (1 μM) in Fura-2 loaded HeLa cells. Data quantifications of rise ratio (340/380 per seconds) after drug treatment were expressed as mean ± S.E., n = 30–50 cells. The \* symbols indicate the results of *t* Test analysis, *p* < 0.05, compared with cells treated with histamine. (B) Kinetics of pHi changes induced by DIEA.HBr (4 mM) and NH<sub>4</sub>Cl (4 mM) in HeLa cells. Data quantifications of indicated pHi changes after drug treatment were expressed as mean ± S.D., *p* < 0.05. (C) ER Ca<sup>2+</sup> concentration, indicated by the thapsigargin (10 μM)-induced Ca<sup>2+</sup> increase, was inhibited by pretreatment of Fura-2 loaded HeLa cells with DIEA.HBr (4 mM) or NH<sub>4</sub>Cl (4 mM) for 7 min or 25 min, but was not affected by ATP (100 μM) or sodium acetate (4 mM) pretreatment. Quantifications of thapsigargin-induced Ca<sup>2+</sup> peaks were expressed as mean ± S.E., n = 30–50 cells, *p* < 0.05 (\*) or *p* < 0.01 (\*\*). (D) Alkaline pH inhibited Ca<sup>2+</sup> uptake capability, whereas thapsigargin (1 μM) abolished Ca<sup>2+</sup> uptake in Fluo-3 loaded permeabilized HeLa cells. Quantifications of Fluo-3 fluorescence at 20 min after drug additions and the decay rate of Fluo-3 fluorescence were expressed as mean ± S.D., *p* < 0.05. All graphs represent data from three independent experiments. doi:10.1371/journal.pone.0031905.g003

sodium orthovanadate, a PMCA inhibitor (Figure S10B) [32], and similar results were observed (Figure S10A). Thus, the slower decay rate of cytosolic Ca<sup>2+</sup> in alkaline pHi is due to the decreased sequestration of cytosolic Ca<sup>2+</sup> to ER, not Ca<sup>2+</sup> extrusion. In addition, it has previously been shown that the ER Ca<sup>2+</sup> refilling via SERCA contributes to Ca<sup>2+</sup> oscillations triggered by ATP in HeLa cells, since co-treatment with thapsigargin abolished the ATP-induced Ca<sup>2+</sup> oscillation. We also found that intracellular alkalinization, similar to thapsigargin, blocked the ATP-induced Ca<sup>2+</sup> oscillation (Figure 4B). Taken together, these data again

demonstrated that intracellular alkalinization inhibits ER SERCA. It is noteworthy that histamine or ATP did not release more Ca<sup>2+</sup>, as indicated by the peak values of the fura 2 fluorescence, whether in the presence or absence of thapsigargin or DIEA.HBr (Figures 4A and 4B). Interestingly, adding thapsigargin (10 μM) right after the peak of Ca<sup>2+</sup> release triggered by DIEA.HBr generated another peak without reducing the subsequent Ca<sup>2+</sup> decay rate, whereas adding DIEA.HBr after the peak of Ca<sup>2+</sup> release evoked by thapsigargin (10 μM) did not produce further Ca<sup>2+</sup> release (Figure S11). Again, these data are consistent with the

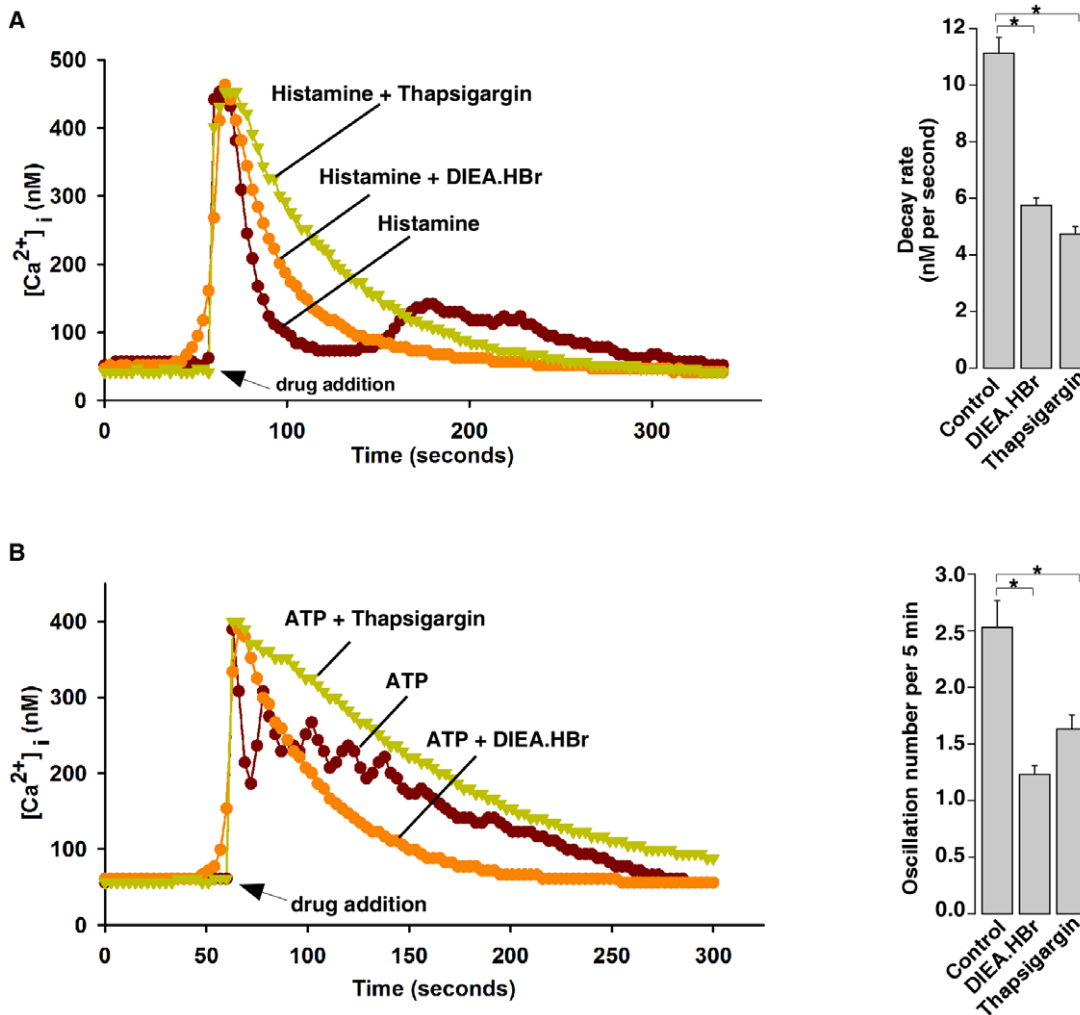


**Figure 4. Intracellular alkalinization inhibits ER Ca<sup>2+</sup> store filling after histamine and ATP treatment in HeLa cells.** (A) Thapsigargin (10 μM) or DIEA.HBr (4 mM) inhibited ER Ca<sup>2+</sup> refilling after histamine (10 μM) treatment in Fura-2 loaded HeLa cells. (B) Thapsigargin (10 μM) or DIEA.HBr (4 mM) diminished ATP (100 μM)-induced Ca<sup>2+</sup> oscillations in Fura-2 loaded HeLa cells. The graphs represent data from three independent experiments, and data quantification are presented as mean ± S.E., n = 9–36 cells. The \* symbols indicate the results of *t* Test analysis, *p* < 0.05. doi:10.1371/journal.pone.0031905.g004

fact that alkalinization partially inhibits SERCA, thereby leading to less extent of Ca<sup>2+</sup> leak from ER than that by higher doses of thapsigargin (Figure 3A).

### Intracellular alkalinization induces Ca<sup>2+</sup> influx by SOC pathway

ER Ca<sup>2+</sup> pool depletion could activate Stim-Orai-mediated SOCs to trigger Ca<sup>2+</sup> influx [11]. Here we have shown above that Ca<sup>2+</sup> influx contributes to the sustained Ca<sup>2+</sup> phase of alkaline pHi-induced Ca<sup>2+</sup> changes (Figure 2A). We, therefore, examined whether the Ca<sup>2+</sup> influx triggered by intracellular alkalinization is via SOCs. Indeed, in NIH 3T3 cells, application of 100 μM La<sup>3+</sup>, an inhibitor of SOCs [33], at the peak of the DIEA.HBr-induced Ca<sup>2+</sup> release in regular HBSS quickly returned Ca<sup>2+</sup> to resting levels (Figure 5A). Similar results have also been observed in several other cell lines (data not shown). Since we have shRNAs against mouse Stim1 and Orai1 on hand, we next knocked down Stim1 or Orai1 in mouse NIH3T3 cells to further examine the role of SOCs in the intracellular alkalinization-induced Ca<sup>2+</sup> influx (Figures 5B and 5C). As expected, thapsigargin (Figure 5D) or intracellular alkalinization (Figures 5E and 5F)-induced Ca<sup>2+</sup> influx was markedly inhibited in Stim1 or Orai1 knockdown cells as compared to that in the control cells. Moreover, when Orai1-EGFP and Stim1-mCherry were co-transfected into HeLa cells, confocal microscopy live cell imaging analysis showed that intracellular alkalinization, similar to thapsigargin, greatly induced the co-localization of Stim1 and Orai1 at the plasma membrane (Figure 6). Taken together, these data clearly indicate that intracellular alkalinization induces Ca<sup>2+</sup> influx via SOCs of Orai1 and Stim1.

### Extracellular alkalinization induces a cytosolic Ca<sup>2+</sup> increase

To further exclude the possibility that SERCA activity might be affected by monovalent cations, such as ammonium or DIEA.H<sup>+</sup>, we used an alternative method to alkalinize pHi by simply raising extracellular pH (Figure 7A) [34]. We found that alkaline extracellular buffer, not acidic buffer, induced cytosolic Ca<sup>2+</sup> increases in HeLa cells (Figure 7B), which were abolished by thapsigargin pretreatment and diminished in a Ca<sup>2+</sup> free medium (Figure 7C). We also examined ER Ca<sup>2+</sup> content at different extracellular pH in HeLa cells (Figure 7D). ER Ca<sup>2+</sup> contents in alkaline pH buffer (8.0, 8.5 and 9.0) were significantly reduced compared to that in the acidified or neutral pH buffers (6.0, 6.5, 7.0 and 7.4). Thus, extracellular alkalinization also triggers cytosolic Ca<sup>2+</sup> release from the ER Ca<sup>2+</sup> pool, as well as induces Ca<sup>2+</sup> influx. In addition, addition of 2 mM Ca<sup>2+</sup> in Ca<sup>2+</sup> free alkaline extracellular buffer induced Ca<sup>2+</sup> increase through influx, which was markedly inhibited in NIH3T3 cells with Stim1 or Orai1 knockdown (Figure 7E), indicating that alkaline pH buffer-triggered Ca<sup>2+</sup> influx is via SOCs as well. In summary, our results indicated that extracellular alkaline buffer triggers cytosolic Ca<sup>2+</sup> increase via intracellular alkalinization as well.

## Discussion

Previous studies on intracellular alkalinization induced Ca<sup>2+</sup> release from intracellular stores suggested that the ER Ca<sup>2+</sup> pools are the main target, yet involvement of IP<sub>3</sub> was a topic of debate [19,23,24]. Studies by Danthuluri et al. also showed that intracellular alkalinization increased Ca<sup>2+</sup> efflux and decreased total cell Ca<sup>2+</sup> concentration in bovine aortic endothelial cells [19]. Here we showed that intracellular alkalinization directly targeted the ER Ca<sup>2+</sup> pools in a wide variety of cell types (Figures 2A and

S4), but blocking two main calcium releasing channels in the ER, IP<sub>3</sub>Rs and RyRs, failed to affect the alkaline pH-induced Ca<sup>2+</sup> release (Figures 2B and 2C). Instead, we found that alkaline pHi inhibited the Ca<sup>2+</sup> refilling activity of ER SERCA, leading to a decrease of the ER Ca<sup>2+</sup> content (Figure 3). The inhibition of the ER Ca<sup>2+</sup> refilling by alkaline pHi was also manifested as the retardation of the decay of the histamine or ATP evoked Ca<sup>2+</sup> transients by intracellular alkalinization (Figure 4). In addition, we showed that the consequence of the alkaline pHi-induced depletion of ER Ca<sup>2+</sup> pools is the activation of extracellular Ca<sup>2+</sup> influx via SOCs of Stim1 and Orai1, which contributes to the sustained elevation of the cytosolic Ca<sup>2+</sup> levels (Figure 5). A previous study also suggested that intracellular alkalinization induces Ca<sup>2+</sup> influx via SOCs [35]. Taken together, we have provided a clear picture of how alkaline pHi increases cytosolic Ca<sup>2+</sup> levels: alkaline pHi inhibits SERCA activity to decrease ER Ca<sup>2+</sup> refilling leading to Ca<sup>2+</sup> leak from ER and lower ER Ca<sup>2+</sup> content, then the partially depleted ER Ca<sup>2+</sup> pools activate SOCs, mediated by Stim1 and Orai1, leading to Ca<sup>2+</sup> influx. The partial depletion of ER Ca<sup>2+</sup> pools by intracellular alkalinization via the inhibition of SERCA is similar to that by lower doses of thapsigargin (Figure S12). Yet, it remains to be determined whether alkaline pH affects some poorly studied or uncharacterized Ca<sup>2+</sup> leak channels located in ER, such as presenilins [36] or sec61 complexes [37].

The molecular mechanisms of intracellular alkalinization induced inhibition of SERCA can be understood from its crystal structures [38,39,40]. SERCAs are transmembrane P-type ATPases that transport cytoplasmic Ca<sup>2+</sup> against its concentration gradient into the lumen of the ER Ca<sup>2+</sup> stores in exchange for luminal protons, at the expense of ATP hydrolysis. During this process, the conformations of SERCAs switch between the E1 and the E2 states, with preference for binding to cytoplasmic Ca<sup>2+</sup> and luminal protons, respectively. The phosphorylation (from ATP) on a conserved aspartate residue locks SERCAs in an E1 state bound with Ca<sup>2+</sup>, while the dephosphorylation of the residue, catalyzed by a conserved TGES motif of the actuator-domain switches SERCAs to a E2 state bound with protons, making them ready for exchanging with cytoplasmic Ca<sup>2+</sup> and starting the next cycle. In cytoplasm, the protonation of a glutamate of the TGES motif is essential for the dephosphorylation of SERCA. It is thus reasonable that intracellular alkalinization could inhibit SERCA by preventing the protonation of the glutamate of the TGES motif at its cytoplasmic region. Inside the ER lumen, four carboxylate residues involved in Ca<sup>2+</sup> binding in the E1 state are also needed to be protonated in order to release the bound Ca<sup>2+</sup> and transit to the E2 state [38,39,40]. It is also possible that intracellular alkalinization by weak bases might increase the pH of the ER lumen, which can easily partition into the ER, thereby preventing the protonation of some of the four Ca<sup>2+</sup> binding-carboxylate groups. This would result in inhibiting counter-transport of protons from inside ER lumen for the cytosolic Ca<sup>2+</sup>. Either way could lock SERCA in the phosphorylated E2 state and stop the pump cycle. Indeed, alkaline pH has been shown to reduce the rate of SERCA dephosphorylation *in vitro* [29]. In addition, Anderden et al showed decades ago that the binding affinity of SERCA for Ca<sup>2+</sup> at alkaline pH was decreased *in vitro* [41].

We found that intracellular alkalinization triggers Ca<sup>2+</sup> entry via SOCs mediated by Orai1 and Stim1 in a wide variety of cells, yet whether alkaline pH directly regulates Orai1 and Stim1 remains to be determined. We have actually found that Ca<sup>2+</sup> influx triggered by thapsigargin is not affected by alkaline pH (Figure S13), suggesting that alkaline pH does not inhibit SOCs. Interestingly, extracellular acidic buffer has been shown to inhibit SOCs,

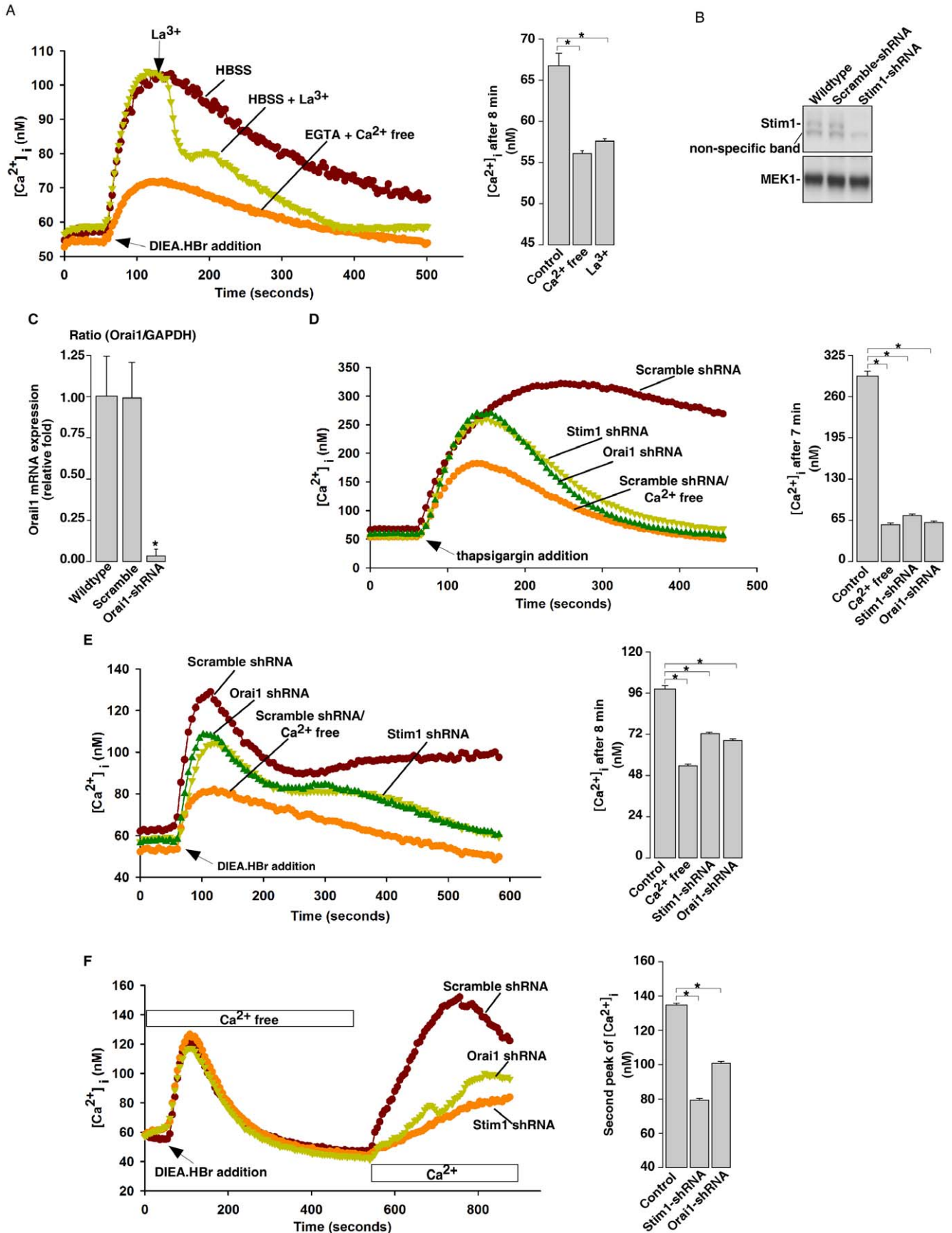




**Figure 5. Intracellular alkalinization induces extracellular Ca<sup>2+</sup> influx through SOCs in NIH 3T3 cells.** (A) DIEA.HBr (4 mM) induced-Ca<sup>2+</sup> influx was inhibited by La<sup>3+</sup> (100 μM), a SOC blocker, treatment in Fura-2 loaded NIH3T3 cells incubated in regular HBSS. (B) Immunoblot analysis of Stim1-knockdown in NIH3T3 cells. GAPDH was used as the internal control. Data are expressed as means ± S.D., n = 3. (C) Quantitative real-time RT-PCR analysis of Orai1-knockdown in NIH3T3 cells. MEK1 immunoblot was used as the internal control. (D) and (E) Stim1 or Orai1 knockdown abolished the sustained Ca<sup>2+</sup> influx induced by thapsigargin (10 μM) (D) and by DIEA.HBr (4 mM) (E) in Fura-2 loaded NIH3T3 cells incubated in regular HBSS. (F) Stim1 and Orai1 knockdown diminished the Ca<sup>2+</sup> influx induced by DIEA.HBr (4 mM) in Fura-2 loaded NIH3T3 cells. Cells were initially treated with thapsigargin (1 μM) in Ca<sup>2+</sup>-free HBSS to deplete ER Ca<sup>2+</sup> pool, followed by 2 mM Ca<sup>2+</sup> addition. All graphs represent data from three independent experiments. Data quantification in (A), (D), (E), and (F) are presented as mean ± S.E., n = 30–50 cells. The \* symbols indicate the results of *t* Test analysis, *p* < 0.05.  
doi:10.1371/journal.pone.0031905.g005

suggesting that protonation of some residues in Orai1 or Stim1 inhibits the gating of SOCs [42].

Besides SOCs, alkaline pH regulates several plasma membrane Ca<sup>2+</sup> channels for Ca<sup>2+</sup> entry [5,15,21,22]. The best known one is the sperm-specific channel, CatSper1, a plasma membrane protein located in the principle piece of the sperm tail. Intracellular alkalinization activates CatSper1 and induces Ca<sup>2+</sup> influx. The result is an increase in the intraflagellar Ca<sup>2+</sup>, which induces hyperactivated sperm motility and is essential for male fertility [5]. In vascular smooth muscle, intracellular alkalinization activates voltage-dependent Ca<sup>2+</sup> channels for Ca<sup>2+</sup> influx and vasoconstriction [3]. Interestingly, alkaline-induced Ca<sup>2+</sup> entry in A7r5 vascular smooth muscle cells also involves a nonselective cation channel and is associated with the concomitant inhibition of voltage-gated Ca<sup>2+</sup> current [43]. We speculate that this non-

selective Ca<sup>2+</sup> channel could be SOCs of Orai1 and Stim1. Along this line, the inhibition of voltage-gated Ca<sup>2+</sup> current by Orai1 and Stim1 has been elegantly illustrated by two recent studies [44,45]. Alkaline pH also activates transient receptor potential (TRP) channel V and A for Ca<sup>2+</sup> entry in neurons, which is related to pain sensation [14,15]. Moreover, it has been shown that the deprotonation of two cysteine residues in TRPA1 is involved in activation by intracellular alkalinization [15]. Besides Ca<sup>2+</sup> channels, pH affects a number of other ion channels, including K<sup>+</sup> channels and aquaporins [46]. Without questions, pHi-dependent modifications on ion channels, structure proteins, or signaling modules, play important roles in regulating their functions.

Even a small change of pH could markedly influence cell behavior, which is why both intra- and extra-cellular pH are tightly regulated. Many physiological and pathological conditions

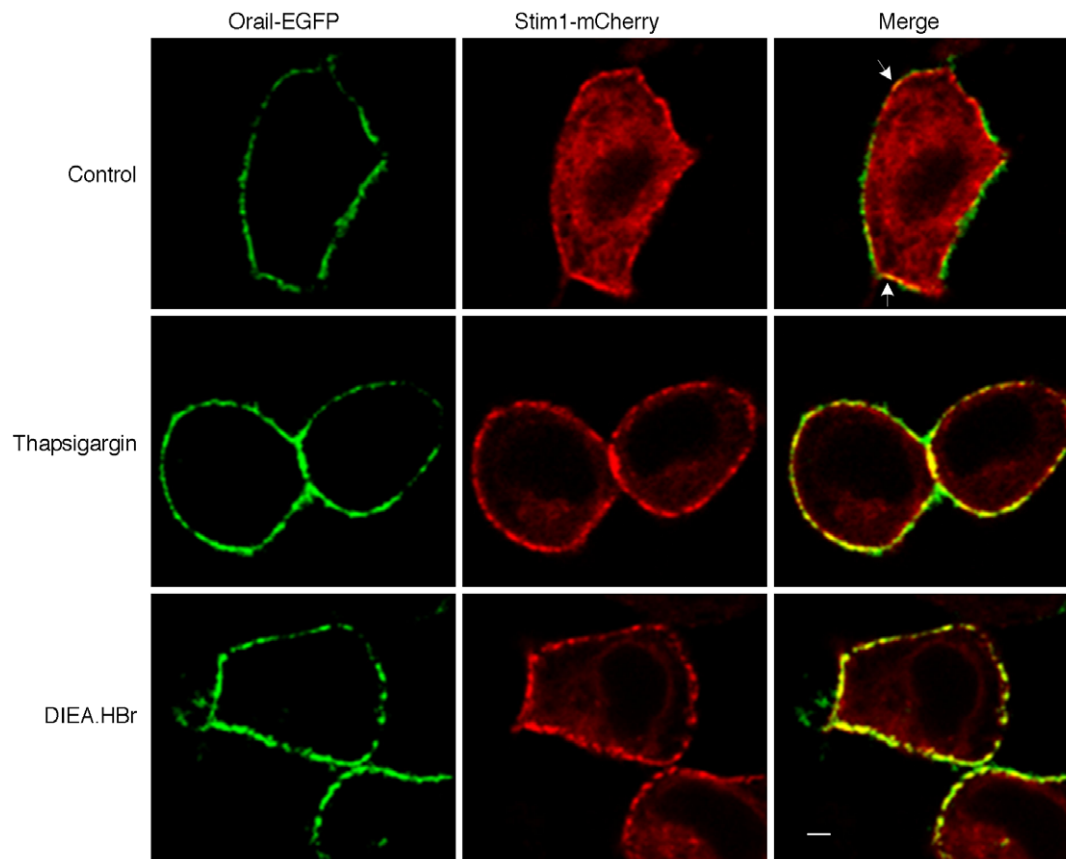


**Figure 6. Intracellular alkalinization induces Stim1 and Orai1 colocalization in HeLa cells.** HeLa cells, co-transfected with plasmids, Stim1-mCherry and Orai1-EGFP, were incubated in Ca<sup>2+</sup> free HBSS for 15 min as control or treated with thapsigargin (10 M) or DIEA.HBr (4 mM) for 15 min in Ca<sup>2+</sup> free HBSS. Confocal imaging of both mCherry and EGFP were taken. The graphs represent data from three independent experiments. Scale bar: 5 μm.  
doi:10.1371/journal.pone.0031905.g006

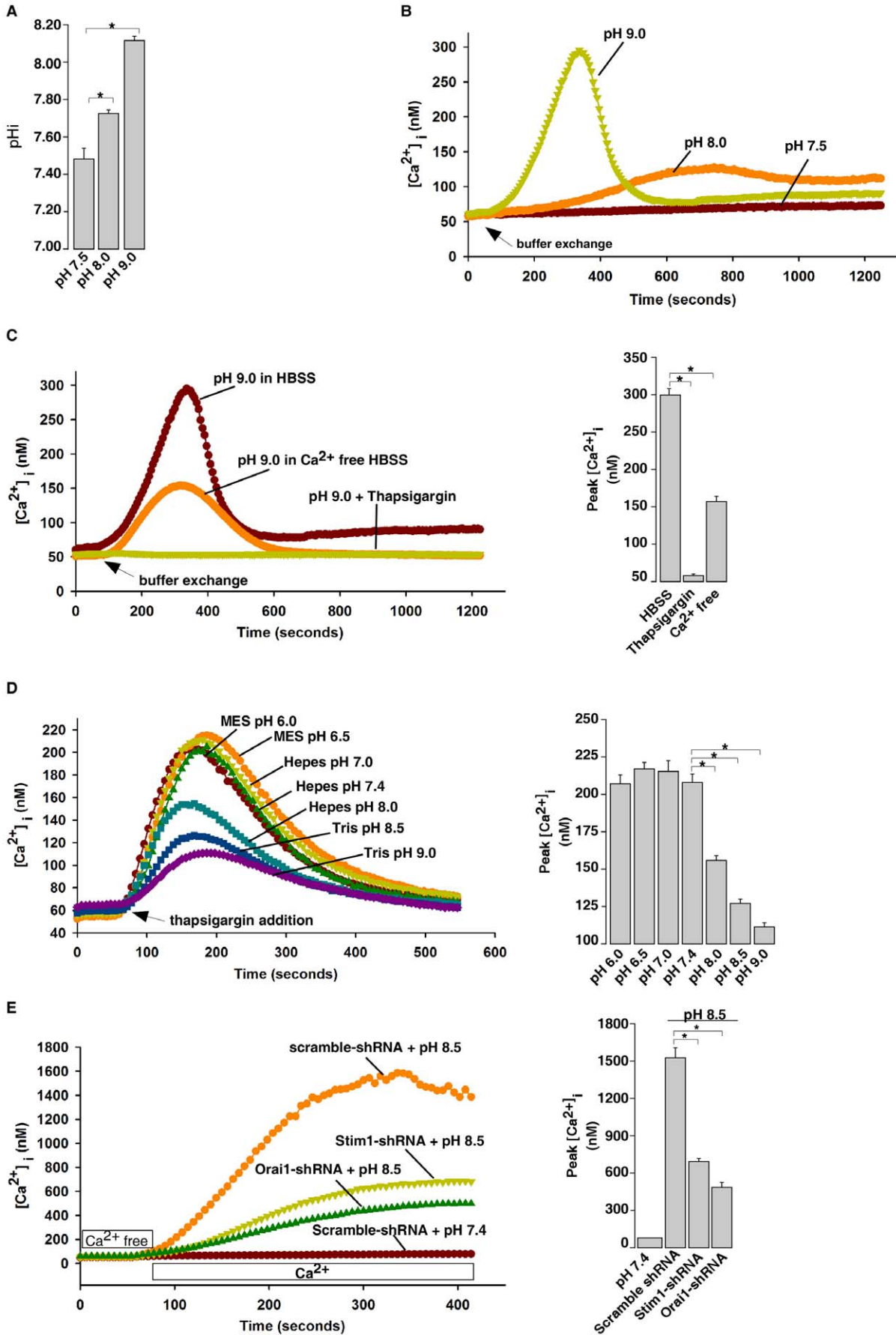


**Figure 7. Extracellular alkalinization induces cytosolic Ca<sup>2+</sup> increases in  $\mu$ HeLa cells and NIH3T3 cells.** (A) Extracellular alkaline buffers induced pH rise in HeLa cells as measured by the pH-indicator, BCECF AM. Data are expressed as means  $\pm$  S.D., n = 3. (B) Extracellular alkaline buffers induced cytosolic Ca<sup>2+</sup> rises in Fura-2 loaded HeLa cells. (C) Extracellular alkaline buffer-induced Ca<sup>2+</sup> increase in Fura-2 loaded HeLa cells was abolished by thapsigargin (1  $\mu$ M) pretreatment or was inhibited by removal of external Ca<sup>2+</sup> (Ca<sup>2+</sup>-free HBSS with 4 mM EGTA). (D) ER Ca<sup>2+</sup> concentration, indicated by the thapsigargin (10  $\mu$ M)-induced Ca<sup>2+</sup> increases, was reduced by extracellular alkaline buffers in HeLa cells. (E) Stim1 or Orai1 knockdown inhibited external Ca<sup>2+</sup> influx induced by extracellular alkaline buffer in NIH3T3 cells. Cells were initially incubated in Ca<sup>2+</sup>-free HBSS with pH adjusted as indicated, followed by 2 mM Ca<sup>2+</sup> addition. All graphs represent data from three independent experiments. Data quantification in (B), (C), (D), and (E) are presented as mean  $\pm$  S.E., n = 30–50 cells. The \* symbols indicate the results of t Test analysis, p < 0.05. doi:10.1371/journal.pone.0031905.g007

produce intra- or extra- cellular alkalinity, which in turn affects a number of cellular processes. Physiologically, intracellular alkalinization has been linked to oocyte maturation, sperm activation, cell proliferation, differentiation, migration, and chemotaxis. Pathologically, intracellular alkalinization is a hallmark of many tumor cells and is associated with tumor progression [47]. It is also well known that hyperventilation induces respiratory alkalosis [48], and both urinary tract infections and irritable bowel symptoms produce high urinary and blood pH [49]. Although pH can directly affect cellular processes by changing the ionization state of proteins, lipids, or other molecules, the secondary effects of pH changes, such as alkalinization-induced cytosolic Ca<sup>2+</sup> increase as described here, on these cellular events should also be taken into consideration. For example, during cell cycle progression, alkalinization induced by NHE activation is required for G2 to M phase transition by unknown mechanisms [7]. Considering Ca<sup>2+</sup> signaling is required for G2 to M transition [50], it is conceivable that intracellular alkalinization could result in cytosolic Ca<sup>2+</sup> spikes, as described in this study, facilitating cell entry into M phase.

Oncogene-dependent overactivation of NHE1 is responsible for intracellular alkalinization in cancer cells, where alkaline pH induces cell proliferation independent of serum. The result is producing poorly vascularized yet dense cell masses, which could in turn create a favorable microenvironment for tumor progression and metastasis [2,51]. It is also well established that Ca<sup>2+</sup> signaling regulates cell proliferation and differentiation. Dysregulation of Ca<sup>2+</sup> contributes to tumor development and metastasis [52]. The results in this study establish a clear mechanistic interrelationship of the pH and Ca<sup>2+</sup> and should provide a valuable framework for investigating the over-activated Ca<sup>2+</sup> signaling activities found in tumors.

## Materials and Methods

### Cell Culture

HeLa, NIH3T3 and 293T cells (*ATCC*) were maintained in DMEM (*Invitrogen*) plus 10% fetal bovine serum (*Invitrogen*) and 100 units/ml of penicillin/streptomycin (*Invitrogen*) at 5% CO<sub>2</sub> and 37°C. PC12 cells (*ATCC*) were maintained in DMEM plus 7.5% horse serum, 7.5% fetal bovine serum, and 100 units/ml of penicillin/streptomycin at 7.5% CO<sub>2</sub> and 37°C. The medium was changed every 48 h.

### Intracellular pH measurement

HeLa cells were cultured in 96-well plates at the density of  $2 \times 10^4$  cells/well in regular medium overnight. Cells were then incubated with 1  $\mu$ M BCECF AM (*Invitrogen*), an intracellular pH indicator, in Hank's balanced salt solution (HBSS) at room temperature for 30 min. Afterwards, cells were washed once with HBSS, and pH<sub>i</sub> of the cells in HBSS at room temperature was measured in TECAN Infinite<sup>®</sup> 200 plate reader in triplicates with excitations set at 440 nm and 490 nm and emission collected at 530 nm every 3 or 10 second. Emission ratios of two different excitations (490 nm/440 nm) were calculated. In addition,

standard intracellular pH curve was obtained by Nigericin/High K<sup>+</sup> method. Briefly, cells in different wells were incubated in calibration buffer (130 mM KCl, 20 mM NaCl, 5 mM hepes and 10  $\mu$ M nigericin) with different pHs, 6.6, 7.0, 7.6 and 8.1. The linear pH standard curve was created with defined buffer pH as X axis and fluorescence ratio (490 nm/440 nm) as Y axis. The intracellular pHs of cells treated with or without drugs were then obtained by calibrating the corresponding 490/440 ratio against the standard curve.

### Intracellular Ca<sup>2+</sup> measurement

Cells were cultured in 24-well plates at the density of  $7 \times 10^4$  cells/well in regular medium overnight and were labeled with 4  $\mu$ M Fura-2 AM (*Invitrogen*) in HBSS at room temperature for 30 min. The cells were then washed with HBSS three times and incubated at room temperature for another 10 min. Cells were put on the stage of an Olympus inverted epifluorescence microscope and visualized using a 20 $\times$  objective. Fluorescence images were obtained by alternate excitation at 340 nm and 380 nm with emission set at 510 nm. Images were collected by a CCD camera every 3 or 6 seconds and analyzed by a *Cell R* imaging software.

### Calcium uptake experiment

Ca<sup>2+</sup> uptake experiments were performed as described previously [53]. Briefly, HeLa cells were trypsinized and washed twice with intracellular buffer (125 mM KCl, 25 mM NaCl, 10 mM Hepes and 0.2 mM MgCl<sub>2</sub>) containing 2 mM EGTA. HeLa cells were then permeabilized with 50  $\mu$ g/mL saponin in intracellular buffer with 2 mM EGTA. Saponin at this concentration only selectively permeabilized the cell membrane while keeping ER membrane intact. The permeabilization efficiency was checked with trypan blue staining, which was typically over 95%. Next, the cells were washed twice in intracellular buffer to remove saponin and EGTA. Finally, permeabilized HeLa cells were suspended in uptake buffers. Uptake buffers were intracellular buffer plus ATP regeneration system (1 mM ATP, 20 mM creatine phosphate, 20 U/mL creatine kinase) with pH adjusted with HCl/KOH to 6.4, 7.2, or 8.0. Fluo-3 salt (4  $\mu$ M) was added to uptake buffers to monitor the calcium change. Fluo-3 fluorescence of permeabilized cells in different uptake buffers at 37°C was measured in TECAN Infinite<sup>®</sup> 200 plate reader with excitation at 488 nm and emission at 526 nm. The fluorescence bleaching was corrected by subtracting the control curve containing no cells.

### Stim1 and Orai1-shRNA lentivirus production and infection

Two optimal 21-mers were selected in the mouse *stim1* and *orai1* gene: CCCTTCGTTTCTTTGCAATAT and CACAACCTCAAC TCGGTCAAA, respectively. Then the two 21-mers were separately subcloned into pLKO.1, a replication- incompetent lentiviral vector for expressing shRNA. Scramble shRNA construct was used as a negative control. 293T cells were used to produce shRNA lentivirus as described previously [25]. For

infection, NIH3T3 cells were plated at density of  $3 \times 10^5$  cells/well in 6-well plates. Next day, 120  $\mu$ l of lentiviruses of stim1 shRNA, orai1 shRNA, or scramble shRNA were added to the cells in fresh medium containing 8  $\mu$ g/ml polybrene. After 24 hrs, cells were selected in fresh medium containing 3  $\mu$ g/ml puromycin for one week. Knockdown efficiency was verified by quantitative real-time RT-PCR or Western blot analysis.

### Quantitative Real-time RT-PCR

The quantitative real-time RT-PCR using the iScript™ One-Step Kit With SYBR® Green (Invitrogen) was performed normally in Bio-Rad MiniOpticon™ Real-Time PCR Detection System according to the manufacture's instructions. The forward primer for orai1 is 5' TCCCTGGTCAGCCATAAGAC and the reverse primer is 5' TCATGGAGAAGGGCATAAAGG. Forward primer for GAPDH is 5' GGACGCATTGGTCG CTGG and reverse primer is 5' TTTGCACTGGTACGTGTTGAT.

### Western Blot Analysis

Control or shRNA-infected NIH3T3 cells were plated at density of  $3 \times 10^5$  cells/well in 6-well plates. Next day, cells were lysed in ice-cold EBC lysis buffer (50 mM Tris-HCl pH8.0, 120 mM NaCl, 0.5% Nonidet P-40, 100  $\mu$ M NaF, 200  $\mu$ M Na<sub>3</sub>VO<sub>4</sub>, 100  $\mu$ g/ml aprotinin, 20  $\mu$ g/ml leupeptin, 150  $\mu$ M phenylmethyl-sulfonyl fluoride, 0.5% sodium deoxy- cholate, and 0.5% SDS). Then the lysates were passed through a 21-gauge needle several times to disperse any large aggregates. Protein concentrations of the cell lysates were determined by the Bradford assay. Proteins (40  $\mu$ g per lane) were diluted in the standard SDS-sample buffer and subjected to electrophoresis on 10% SDS polyacrylamide gels. Proteins were transferred to an Immobilon-P blotting membrane (Millipore), blocked with 5% milk in Tris-buffered saline (20 mM Tris, 150 mM NaCl, pH 7.6) with 0.1% Tween 20, and incubated with primary antibody against Stim1 (BD Biosciences, 1:1000 dilution) for 2.5 h. After washing, the blots were probed with a secondary antibody for detection by chemiluminescence.

### Stim1-mCherry and Orai1-EGFP colocalization

Two plasmids, *pStim1-mCherry* and *pOrai1-EGFP*, were provided by Dr. Gwack, Y [54]. HeLa cells were plated on coverslips in 6-well plates at density of  $3 \times 10^5$  cells/well. Next day, *pStim1-mCherry* and *pOrai1-EGFP* were co-transfected into HeLa cells by Lipofectamine™ 2000. 48 hours after transfection, cells were washed twice with Ca<sup>2+</sup> free HBSS. Distributions of Stim1 and Orai1 in transfected cells at room temperature were then examined in Ca<sup>2+</sup> free HBSS containing thapsigargin or DIEA.HBr by confocal laser-scanning microscopy (Olympus FV300) with an Olympus PlanApo 60 $\times$  Oil objective.

### Supporting Information

**Figure S1 Purification of DIEA.HBr.** (A) HPLC fractionation of an esterification reaction. DIEA.HBr was purified in fraction 7. (B) Chemical structure of DIEA.HBr. (C) DIEA.HBr crystals were obtained by recrystallization method. (D) H-NMR of DIEA.HBr. (E) C-NMR of DIEA.HBr.

**Figure S2 NaBr (4 mM) and KBr (4 mM) cannot induce any cytosolic Ca<sup>2+</sup> change compared with the effect of DIEA.HBr (4 mM).** The graphs represent data from three independent experiments.

**Figure S3 DIEA.HBr induces cytosolic pH increase in a dose dependent manner in HeLa cells.** The graphs represent data from three independent experiments.

**Figure S4 Intracellular alkalinization induced by DIEA.HBr (4 mM) releases Ca<sup>2+</sup> from ER pools in various cell types, including D3 mouse embryonic stem cells (A), NIH3T3 fibroblasts (B), BHK21 fibroblasts (C), HEK293T cells (D), HL 60 leukemic cells (E), PC 12 cells (F), Jurkat T lymphocyte cells (G), and THP-1 leukemic cells (H).** The graphs represent data from three independent experiments.

**Figure S5 The effectiveness of Xestospingin C, U73122, and ryanodine.** (A) Histamine (10  $\mu$ M) induced Ca<sup>2+</sup> rise was markedly inhibited by *Xestospingin C* (10  $\mu$ M, 30 min pretreatment) and U73122 (10  $\mu$ M, 15 min pretreatment). (B) Ryanodine (20  $\mu$ M, 30 min pretreatment) blocked caffeine (10 mM) induced Ca<sup>2+</sup> rise in PC 12 cells whereas caffeine failed to induce Ca<sup>2+</sup> increases in HeLa cells.

**Figure S6 Complete depletion of lysosomal Ca<sup>2+</sup> pools by GPN (50  $\mu$ M) in HeLa cells.** Fura-2 loaded HeLa cells were treated with GPN (50  $\mu$ M) to released lysosomal Ca<sup>2+</sup>. Subsequent addition of GPN (50  $\mu$ M) or bafilomycin A1(0.5  $\mu$ M) failed to release any more Ca<sup>2+</sup>.

**Figure S7 Inhibition of SERCA ATPase activities by alkaline buffers in vitro.** Top: HEK 293T cell lysates (300  $\mu$ g) were incubated with anti-SERCA3 antibody (PL/IM430, *Sigma*) pre-bound to protein G beads. The SERCA3 immunocomplexes were then washed by TBS and separated evenly into three different pH Tris buffer (100 mM) at pH 7.5, 8.5, and 9.5, respectively. The ATPase activity of the immunocomplexes in different pH buffers were finally measured by a colorimetric assay for ATPase (*Innova Bioscience*) in a 96-well format and done in triplicates. As a control, boiling the immunocomplexes completely killed the ATPase activity. The graphs represent data from three independent experiments, and data quantification are presented as mean  $\pm$  S.D., n = 3. Bottom: *Western blot* analysis of SERCA3 in SERCA3 IP complexes in indicated buffers after ATPase assay.

**Figure S8 Intracellular alkalinization induced by DIEA.HBr decreases ionomycin-releasable Ca<sup>2+</sup> pool in HeLa cells.** After 7 min of DIEA.HBr (4 mM) or MQ pretreatment, ionomycin (5  $\mu$ M) was used to examine intracellular Ca<sup>2+</sup> pool content in Ca<sup>2+</sup> free HBSS containing 2 mM EGTA. The graphs represent data from three independent experiments. Quantifications of ionomycin-induced Ca<sup>2+</sup> peaks were expressed as mean  $\pm$  S.E., n = 30–50 cells, *p* < 0.05.

**Figure S9 Alkaline pH inhibits thapsigargin-sensitive Ca<sup>2+</sup> uptake capability in HeLa cells in uptake buffer containing ruthenium red.** Quantifications of Fluo-3 fluorescence at 25 min after drug additions were expressed as mean  $\pm$  S.D., *p* < 0.05. All graphs represent data from three independent experiments.

**Figure S10 Intracellular alkalinization inhibits ER Ca<sup>2+</sup> store filling after histamine treatment in the presence of a PMCA inhibitor.** (A) Thapsigargin (10  $\mu$ M) or DIEA.HBr

(4 mM) inhibited ER Ca<sup>2+</sup> refilling after histamine (10 μM) treatment in HeLa cells in the presence of sodium orthovanadate (5 mM), a PMCA inhibitor. (B) HeLa cells were first over-loaded with Ca<sup>2+</sup> by extracellular Ca<sup>2+</sup> (2 mM) and ionomycin (10 μM) addition. Then the buffer was changed to Ca<sup>2+</sup> free HBSS, and the removal of over-loaded intracellular Ca<sup>2+</sup> was significantly inhibited in the presence of sodium orthovanadate (5 mM) compared with that in control. (PDF)

**Figure S11 Intracellular alkalinization partially depletes ER Ca<sup>2+</sup> pools in HeLa cells.** Treating the cell with DIEA.HBr (4 mM) around the peak of Ca<sup>2+</sup> curve induced by thapsigargin (10 μM) failed to cause additional Ca<sup>2+</sup> rise, whereas adding thapsigargin (10 μM) around the peak induced by DIEA.HBr (4 mM) triggered another Ca<sup>2+</sup> rise. The graphs represent data from three independent experiments. (PDF)

**Figure S12 The partial inhibition of SERCA by lower doses of thapsigargin results in partial depletion of ER Ca<sup>2+</sup> content and subsequent cytosolic Ca<sup>2+</sup> increase in HeLa cells.** (A) ER Ca<sup>2+</sup> concentration, indicated by the thapsigargin (10 μM)-induced Ca<sup>2+</sup> increase, was inhibited by pretreatment of Fura-2 loaded HeLa cells with 10 nM thapsigargin.

(B) 10 nM thapsigargin also directly induced cytosolic Ca<sup>2+</sup> increase in HeLa cells. (PDF)

**Figure S13 Intracellular alkalinization has no effect on SOCE pathway induced by thapsigargin.** In Ca<sup>2+</sup> free HBSS, thapsigargin (10 μM) was used to completely deplete ER Ca<sup>2+</sup> pool, then intracellular alkalinization was induced by applying DIEA.HBr (4 mM). The amplitude of Ca<sup>2+</sup> influx during intracellular alkalinization exhibited no significant differences compared with that in control. The graphs represent data from three independent experiments. (PDF)

## Acknowledgments

We thank Rich Graeff and other members of Yue and Lee labs for advice on the manuscript.

## Author Contributions

Conceived and designed the experiments: SL JBY. Performed the experiments: SL BXH YYL PLY. Analyzed the data: SL BXH YYL PLY. Contributed reagents/materials/analysis tools: SL BXH YYL PLY. Wrote the paper: SL HCL JBY.

## References

- Casey JR, Grinstein S, Orlowski J (2010) Sensors and regulators of intracellular pH. *Nature Reviews Molecular Cell Biology* 11: 50–61.
- Srivastava J, Barber DL, Jacobson MP (2007) Intracellular pH sensors: design principles and functional significance. *Physiology* 22: 30–39.
- Wakabayashi I, Poteser M, Groschner K (2006) Intracellular pH as a determinant of vascular smooth muscle function. *Journal of vascular research* 43: 238–250.
- Lyall V, Biber TU (1994) Potential-induced changes in intracellular pH. *The American journal of physiology* 266: F685–696.
- Kirichok Y, Navarro B, Clapham DE (2006) Whole-cell patch-clamp measurements of spermatozoa reveal an alkaline-activated Ca<sup>2+</sup> channel. *Nature* 439: 737–740.
- Nuccitelli R, Webb DJ, Lagier ST, Matson GB (1981) P-31 NMR REVEALS INCREASED INTRACELLULAR PH AFTER FERTILIZATION IN XENOPUS EGGS. *Proceedings of the National Academy of Sciences of the United States of America-Biological Sciences* 78: 4421–4425.
- Putney LK, Barber DL (2003) Na-H exchange-dependent increase in intracellular pH times G<sub>2</sub>/M entry and transition. *Journal of Biological Chemistry* 278: 44645–44649.
- Putney LK, Denker SP, Barber DL (2002) The changing face of the Na<sup>+</sup>/H<sup>+</sup> exchanger, NHE1: structure, regulation, and cellular actions. *Annual review of pharmacology and toxicology* 42: 527–552.
- Lee HC (2004) Multiplicity of Ca<sup>2+</sup> messengers and Ca<sup>2+</sup> stores: a perspective from cyclic ADP-ribose and NAADP. *Curr Mol Med* 4: 227–237.
- Clapham DE (2007) Calcium signaling. *Cell* 131: 1047–1058.
- Cahalan MD (2009) STIMulating store-operated Ca<sup>2+</sup> entry. *Nature cell biology* 11: 669–677.
- Epel D (1978) Mechanisms of activation of sperm and egg during fertilization of sea urchin gametes. *Current topics in developmental biology* 12: 185–246.
- Epel D (1978) Regulation of cell activity at fertilization by intracellular Ca<sup>2+</sup> and intracellular pH. *Birth defects original article series* 14: 377–388.
- Dhaka A, Uzzell V, Dubin AE, Mathur J, Petrus M, et al. (2009) TRPV1 is activated by both acidic and basic pH. *The Journal of neuroscience : the official journal of the Society for Neuroscience* 29: 153–158.
- Fujita F, Uchida K, Moriyama T, Shima A, Shibasaki K, et al. (2008) Intracellular alkalinization causes pain sensation through activation of TRPA1 in mice. *The Journal of clinical investigation*.
- Speake T, Elliott AC (1998) Modulation of calcium signals by intracellular pH in isolated rat pancreatic acinar cells. *The Journal of physiology* 506(Pt 2): 415–430.
- Heppner TJ, Bonev AD, Santana LF, Nelson MT (2002) Alkaline pH shifts Ca<sup>2+</sup> sparks to Ca<sup>2+</sup> waves in smooth muscle cells of pressurized cerebral arteries. *American journal of physiology Heart and circulatory physiology* 283: H2169–2176.
- Alfonso A, Cabado AG, Vieytes MR, Botana LM (2000) Calcium-pH crosstalks in rat mast cells: cytosolic alkalinization, but not intracellular calcium release, is a sufficient signal for degranulation. *British journal of pharmacology* 130: 1809–1816.
- Danthuluri NR, Kim D, Brock TA (1990) INTRACELLULAR ALKALINIZATION LEADS TO CA<sup>2+</sup> MOBILIZATION FROM AGONIST-SENSITIVE POOLS IN BOVINE AORTIC ENDOTHELIAL-CELLS. *Journal of Biological Chemistry* 265: 19071–19076.
- Cabado AG, Alfonso A, Vieytes MR, Gonzalez M, Botana MA, et al. (2000) Crosstalk between cytosolic pH and intracellular calcium in human lymphocytes: effect of 4-aminopyridin, ammonium chloride and ionomycin. *Cellular signalling* 12: 573–581.
- Poteser M, Wakabayashi I, Rosker C, Teubl M, Schindl R, et al. (2003) Crosstalk between voltage-independent Ca<sup>2+</sup> channels and L-type Ca<sup>2+</sup> channels in A7r5 vascular smooth muscle cells at elevated intracellular pH - Evidence for functional coupling between L-type Ca<sup>2+</sup> channels and a 2-APB-sensitive cation channel. *Circulation Research* 92: 888–896.
- Klockner U, Isenberg G (1994) INTRACELLULAR PH MODULATES THE AVAILABILITY OF VASCULAR L-TYPE CA<sup>2+</sup> CHANNELS. *Journal of General Physiology* 103: 647–663.
- Tsukioka M, Ino M, Endo M (1994) PH-DEPENDENCE OF INOSITOL 1,4,5-TRISPHOSPHATE-INDUCED CA<sup>2+</sup> RELEASE IN PERMEABILIZED SMOOTH-MUSCLE CELLS OF THE GUINEA-PIG. *Journal of Physiology-London* 475: 369–375.
- Leffler CW, Balabanova L, Williams KK (1999) cAMP production by piglet cerebral vascular smooth muscle cells: pH(o), pH(i), and permissive action of PGI<sub>2</sub>. *The American journal of physiology* 277: H1878–1883.
- Yue JB, Wei WJ, Lam CMC, Zhao YJ, Dong M, et al. (2009) CD38/cADPR/Ca<sup>2+</sup> Pathway Promotes Cell Proliferation and Delays Nerve Growth Factor-induced Differentiation in PC12 Cells. *Journal of Biological Chemistry* 284: 29335–29342.
- Jadot M, Andrianaivo F, Dubois F, Wattiaux R (2001) Effects of methylcyclodextrin on lysosomes. *European Journal of Biochemistry* 268: 1392–1399.
- Srinivas SP, Ong A, Goon L, Bonanno JA (2002) Lysosomal Ca<sup>2+</sup> stores in bovine corneal endothelium. *Investigative Ophthalmology & Visual Science* 43: 2341–2350.
- Olesen C, Sorensen TL, Nielsen RC, Moller JV, Nissen P (2004) Dephosphorylation of the calcium pump coupled to counterion occlusion. *Science* 306: 2251–2255.
- Sorensen T, Vilsen B, Andersen JP (1997) Mutation Lys(758)→Ile of the sarcoplasmic reticulum Ca<sup>2+</sup>-ATPase enhances dephosphorylation of E2P and inhibits the E-2 to E1Ca<sub>2</sub> transition. *Journal of Biological Chemistry* 272: 30244–30253.
- Crepin A, Bidaux G, Vanden-Abeece F, Dewailly E, Goffin V, et al. (2007) Prolactin stimulates prostate cell proliferation by increasing endoplasmic reticulum content due to SERCA 2b over-expression. *Biochemical Journal* 401: 49–55.
- Kargacin GJ, Aschar-Sobbi R, Kargacin ME (2005) Inhibition of SERCA2 Ca<sup>2+</sup>-ATPases by Cs<sup>+</sup>. *Pflugers Archiv-European Journal of Physiology* 449: 356–363.
- Lajas AI, Sierra V, Camello PJ, Salido GM, Pariente JA (2001) Vanadate inhibits the calcium extrusion in rat pancreatic acinar cells. *Cellular signalling* 13: 451–456.

33. Kapur N, Mignery GA, Banach K (2007) Cell cycle-dependent calcium oscillations in mouse embryonic stem cells. *American Journal of Physiology-Cell Physiology* 292: C1510–C1518.
34. Austin C, Dilly K, Eisner D, Wray S (1996) Simultaneous measurement of intracellular pH, calcium, and tension in rat mesenteric vessels: Effects of extracellular pH. *Biochemical and Biophysical Research Communications* 222: 537–540.
35. Nitschke R, Riedel A, Ricken S, Leipziger J, Benning N, et al. (1996) The effect of intracellular pH on cytosolic Ca<sup>2+</sup> in HT29 cells. *Pflügers Archiv-European Journal of Physiology* 433: 98–108.
36. Tu HP, Nelson O, Bezprozvanny A, Wang ZN, Lee SF, et al. (2006) Presenilins form ER Ca<sup>2+</sup> leak channels, a function disrupted by familial Alzheimer's disease-linked mutations. *Cell* 126: 981–993.
37. Lang S, Erdmann F, Jung M, Wagner R, Cavalie A, et al. (2011) Sec61 complexes form ubiquitous ER Ca(2+) leak channels. *Channels* 5: 228–235.
38. Toyoshima C, Nomura H, Tsuda T (2004) Lumenal gating mechanism revealed in calcium pump crystal structures with phosphate analogues. *Nature* 432: 361–368.
39. Olesen C, Sorensen TLM, Nielsen RC, Moller JV, Nissen P (2004) Dephosphorylation of the calcium pump coupled to counterion occlusion. *Science* 306: 2251–2255.
40. Sorensen TL, Moller JV, Nissen P (2004) Phosphoryl transfer and calcium ion occlusion in the calcium pump. *Science* 304: 1672–1675.
41. Andersen JP, Lassen K, Moller JV (1985) CHANGES IN CA-2+ AFFINITY RELATED TO CONFORMATIONAL TRANSITIONS IN THE PHOSPHORYLATED STATE OF SOLUBLE MONOMERIC CA-2+-ATPASE FROM SARCOPLASMIC-RETICULUM. *Journal of Biological Chemistry* 260: 371–380.
42. Marumo M, Suhiro A, Kakishita E, Groschner K, Wakabayashi I (2001) Extracellular pH affects platelet aggregation associated with modulation of store-operated Ca(2+) entry. *Thrombosis research* 104: 353–360.
43. Poteser M, Wakabayashi I, Rosker C, Teubl M, Schindl R, et al. (2003) Crosstalk between voltage-independent Ca<sup>2+</sup> channels and L-type Ca<sup>2+</sup> channels in A7r5 vascular smooth muscle cells at elevated intracellular pH: evidence for functional coupling between L-type Ca<sup>2+</sup> channels and a 2-APB-sensitive cation channel. *Circulation research* 92: 888–896.
44. Wang Y, Deng X, Mancarella S, Hendron E, Eguchi S, et al. (2010) The calcium store sensor, STIM1, reciprocally controls Orai and CaV1.2 channels. *Science* 330: 105–109.
45. Park CY, Shcheglovitov A, Dolmetsch R (2010) The CRAC channel activator STIM1 binds and inhibits L-type voltage-gated calcium channels. *Science* 330: 101–105.
46. Navarro B, Kirichok Y, Clapham DE (2007) KSper, a pH-sensitive K<sup>+</sup> current that controls sperm membrane potential. *Proceedings of the National Academy of Sciences of the United States of America* 104: 7688–7692.
47. Reshkin SJ, Bellizzi A, Caldeira S, Albarani V, Malanchi I, et al. (2000) Na<sup>+</sup>/H<sup>+</sup> exchanger-dependent intracellular alkalinization is an early event in malignant transformation and plays an essential role in the development of subsequent transformation-associated phenotypes. *FASEB Journal* 14: 2185–2197.
48. Mogyoros I, Kiernan MC, Burke D, Bostock H (1997) Excitability changes in human sensory and motor axons during hyperventilation and ischaemia. *Brain: a journal of neurology* 120(Pt 2): 317–325.
49. Cohen PG (1984) The hypokalemic, bowel, bladder, headache relationship; a new syndrome. The role of the potassium ammonia axis. *Medical hypotheses* 15: 135–140.
50. Whitaker M (2006) Calcium at fertilization and in early development. *Physiological reviews* 86: 25–88.
51. Paradiso A, Cardone RA, Bellizzi A, Bagorda A, Guerra L, et al. (2004) The Na<sup>+</sup>-H<sup>+</sup> exchanger-1 induces cytoskeletal changes involving reciprocal RhoA and Rac1 signaling, resulting in motility and invasion in MDA-MB-435 cells. *Breast cancer research: BCR* 6: R616–628.
52. Muller MR, Rao A (2010) NFAT, immunity and cancer: a transcription factor comes of age. *Nature reviews Immunology* 10: 645–656.
53. Tengholm A, Hellman B, Gylfe E (2000) Mobilization of Ca<sup>2+</sup> stores in individual pancreatic beta-cells permeabilized or not with digitonin or alpha-toxin. *Cell calcium* 27: 43–51.
54. Srikanth S, Jung HJ, Kim KD, Souda P, Whitelegge J, et al. (2010) A novel EF-hand protein, CRACR2A, is a cytosolic Ca<sup>2+</sup> sensor that stabilizes CRAC channels in T cells. *Nature Cell Biology* 12: 436–U463.